Proceedings of the 13th Asian Congress of Fluid Mechanics
17-21 December 2010, Dhaka, Bangladesh

Scaling Laws in Vortex Reconnection

Fazle Hussain[1], Karthik Duraisamy[2]
[1] Department of Mechanical Engineering, University of Houston, Houston, USA.
[2] Department of Aeronautics and Astronautics, Stanford University, Stanford, USA.

E-mail of presenting author: fhussain@houston.edu

Abstract This work is motivated by our long-standing claim that reconnection of coherent structures is the dominant mechanism of jet noise generation and plays a key role in both energy cascade and fine-scale mixing in fluid turbulence (Hussain 1983, 1986). To shed further light on the mechanism involved and quantify its features, reconnection of two anti-parallel vortex tubes is studied by direct numerical simulation of the incompressible Navier-Stokes equations over a wide range (250-9000) of the vortex Reynolds number, Re (= circulation/viscosity) at much higher resolutions than have been attempted. Unlike magnetic or superfluid reconnections, viscous reconnection is never complete, leaving behind a part of the initial tubes as âĽ˜threadsâĽ™, which then undergo successive reconnections (our cascade and mixing scenarios) as the newly formed âĽ˜bridgesâĽ™ recoil from each other by self-advection. We find that the time t_R for orthogonal transfer of circulation scales as $t_R \approx Re^{-3/4}$. The shortest distance d between the tube centroids scales as $d \approx a(Re(t_0 - t))^{3/4}$ before reconnection (collision) and as $d \approx b(Re(t - t_0))^2$ after reconnection (repulsion), where t_0 is the instant of smallest separation between vortex centroids. We find that b is a constant, thus suggesting self-similarity, but a is dependent on Re. Bridge repulsion is faster than collision and is more autonomous as local induction predominates, and given the associated acceleration of vorticity, is potentially a source of intense sound generation. At the higher Re's studied, the tails of the colliding threads are compressed into a planar jet with multiple vortex pairs. For $Re > 6000$, there is an avalanche of smaller scales during the reconnection - the rate of small scale generation and the spectral content (in vorticity, transfer function and dissipation spectra) being quite consistent with the structures visualized by the λ_2 criterion. The maximum rate of vortex circulation transfer, enstrophy production and dissipation scale as $Re^1, Re^{7/4}, Re^{-1/2}$, respectively. A more detailed study of subsequent reconnection of threads requires much higher-resolution simulations that are currently not feasible.

Keywords Vortex reconnection, Coherent structures, Turbulent cascade

1. Background

There is now considerable renewed interest in vortex reconnection, not only in viscous vortices, but also in quantized vortices - the similarities and differences between them have been recently reviewed [1]. Although explored before, the viscous reconnection mechanism and its quantitative characterization have remained vague [2]. We attempt to shed further light on this mechanism - long suggested by us to be the essence of mixing and cascade in turbulent flows. Our interest in reconnection arose from our search and suggestion for the mechanisms of jet noise generation. Refuting the prevalent suggestion that vortex pairing was the primary source of jet noise [3-6], Hussain & Zaman [7,8] asserted that it must be the reconnection of the underlying lobed vortex rings into satellite rings - an abrupt viscous process involving topological transformation - that produce most jet noise. Hussain further claimed [9,10] that reconnection of vortex filaments was the essential element of turbulence cascade and fine-scale mixing. Although a

number of studies [11-16] have addressed the viscous reconnection problem, both the underlying mechanism and various scaling relationships have remained elusive. We present here some of the important scaling relations and explanations of the mechanisms.

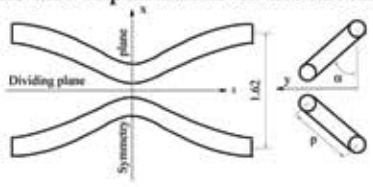

Figure 1: Initial configuration

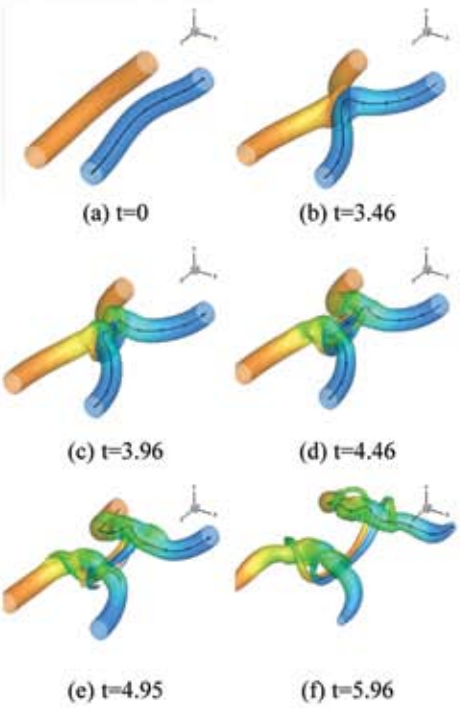

(a) t=0 (b) t=3.46

(c) t=3.96 (d) t=4.46

(e) t=4.95 (f) t=5.96

Figure 2: Vorticity magnitude iso-surfaces at 40% of maximum initial vorticity (colored with contours of axial vorticity) for Re=2000

2. Problem setup

To focus on the basic mechanism of reconnection, we adopt a simple initial condition similar to that used by Melander & Hussain [15]. Two anti-parallel vortex tubes are initialized in the flow with a symmetric perturbation to the vortex axes (Fig. 1). The computational domain is a cube of side 2π, with $z=0$ being the symmetry plane and the vortex axes being nominally aligned with the z-axis. The position of the vortex centroid is given by $\mathbf{r}=\{x_c+p\cos\alpha f(z), y_c+p\sin\alpha f(z)\}$, where (x_c,y_c) is the position of the unperturbed vortex centroid, p is the amplitude of the perturbation, α is the angle of the vortex axis with respect to the x-axis and $f(z)$ is the form of the perturbation. A divergence-free vorticity field is then specified as $\omega=\omega_0(r/r_c)[a\cos\alpha f'(z), a\sin\alpha f', 1]$ where $\omega_0(r)$ is a compact Gaussian distribution (for $r<r_c$) as detailed in Melander and Hussain. In the present work, $(x_c,y_c)=(\pm 0.81,0)$, $\alpha=60°$, $r_c=0.666$, $p=0.2$ and $f(z)=cos(z)$. Several simulations were performed for Reynolds numbers (defined as $Re=\Gamma_z/\nu$, where Γ_z is the circulation of each vortex tube and ν is the kinematic viscosity) of 250, 500, 1000, 2000, 4000, 6000, 7500 and 9000.

A pseudo-spectral formulation of the vorticity transport equations[16] is used for the flow solution with grid convergence assessed by monitoring pile up of spectra and by repeating every calculation on a mesh that is 1.25 times as coarse in each direction. The mesh sizes ranged from 64^3 to 1024^3.

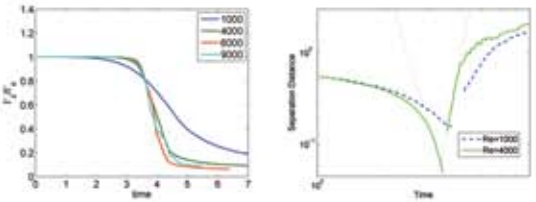

(a) Evolution of axial Circulation (b) Vortex separations before and after reconnection

Figure 3: Time evolution

3. Physics of reconnection

Figure 1 accentuates the initial sinusoidal displacement and tilting of the tubes, designed to assure that the two will collide with each other by self-induction, thus initiating and sustaining reconnection. Also shown is the coordinate system and the symmetry $(x-y)$ and dividing $(y-z)$ planes. Figure 2 shows the time progression of the reconnection. The rate of flattening, evident in Fig. 2b, increases with *Re*; the

resolution of this structure was found to limit computations at very high *Re*. Note that in the inviscid limit, the vortex cores can be expected to be pressed into infinitesimally thin vortex sheets as suggested in Ref. [17]. As a comparison with that work, the finest mesh resolution in the present work was around 1% of the vortex core diameter which is about 3 times coarser than the finest mesh used in the *inviscid* simulations of Ref. [17]. At the point of contact between the two tubes, adjacent vortex lines belonging to the two tubes cancel each other by viscous cross-diffusion connecting the remainder of the lines on either end of the region. The sharp corner at the reconnected points at both ends of the annihilated part recede rapidly away from each other and also curl up (by curvature-induced self-advection), while being stretched by the continuing rotation of the tubes and then laid orthogonal to the tubes atop them. Successive reconnected lines are likewise stretched and laid on top of the prior vortex lines, orthogonal to the initial tubes - the genesis of the bridges. The corresponding circulation transfer (loss) from the axial direction to the orthogonal direction is shown in fig. 3a. The cross diffusion is caused by the vorticity gradient close to the symmetry plane, intensified by collision and stretching. Note that interpretations in terms of vortex lines have to be reconciled with viscous effects and in fact vortex lines may not necessarily stay near the center of the core even in inviscid flows[18]. As the hairpin-shaped bridges get stronger with increasing transferred circulations, self induction causes them to retract from the interaction region. This action also progressively stretches the remainder (the threads) of the tubes while simultaneously reversing their curvature by the jet between the two bridges. This reversal makes the two threads move away from each other, thus slowing the circulation transfer and actually arresting the reconnection process.

When the bridges have moved sufficiently far apart, however, mutual induction between the two adjacent threads would overcome the thrust of the weakened jet of the bridge pair, reversing their curvature, again, at the point halfway between the bridges. This will cause the two threads to collide again, starting the next round of reconnection. The process thus will repeat again (if *Re* is high enough) and is the proposed reconnection cascade scenario. There is a second facet of the reconnection: fine-scales triggered at the thread-bridge junction, particularly at higher *Re*. Note the reorientation of the vortex line passing through the vortex center at the end between Figs. 2c,d. Although the threads are clear, their imminent second reconnection is apparent from Fig. 2f. The heightened deformation of the vortex lines leading to the topology changing reconnection event is evident. Also, the vortex lines passing through the centers of the threads are intensely stretched (see at $t = 4.46$), leading to an array of small scale structures, especially at higher *Re*.

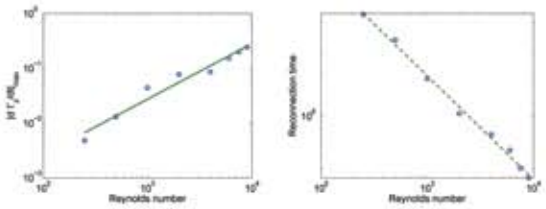

(a) Max rate of change of circulation $\approx cRe$ (b) Reconnection time $\approx dRe^{-0.75}$

Figure 4: Circulation transfer metrics

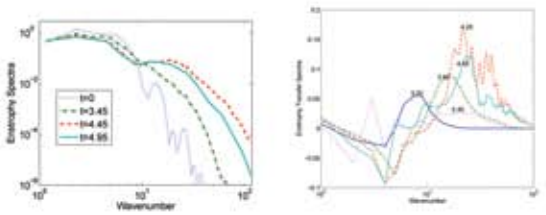

(a) Enstrophy (b) Enstrophy Transfer

Figure 5: Spectra for Re=2000

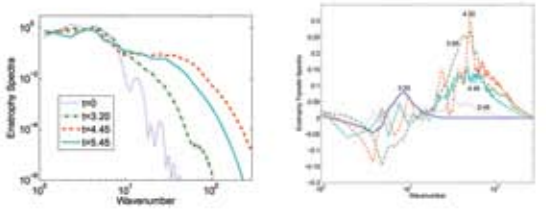

(a) Enstrophy (b) Enstrophy Transfer

Figure 6: Spectra for Re=6000

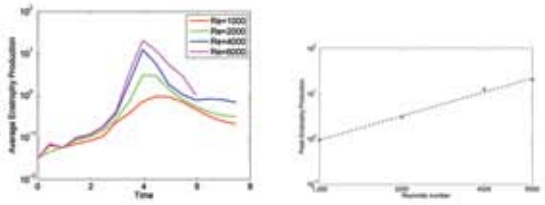

(a) Enstrophy Production (b) Peak Enstrophy Production

Figure 7: Evolution of volume averaged enstrophy production

4. Scaling with Reynolds number

A particularly interesting question is the evolution of the separation distance between the tubes and bridges. Figure 3b shows this separation at two representative Reynolds numbers. Unlike in magnetic or superfluid reconnections, where each reconnection is complete with no threads, and hence the separation between the tubes and bridges is clear, here separation distance cannot be sharply defined. The tubes undergo significant core deformation before reconnection, and the reconnected vortex filaments take some time to collect together to form the bridge. In both stages, the vorticity is distributed in irregular shapes without any clear vortex center. We thus take the vorticity centroid (taken to be the centroid of all vorticity that is above 75% of the maximum vorticity) to be the location of the tubes and bridges. With this caveat, the time for reconnection can be fairly accurately defined. The separation d between the tubes was found to scale as $d \approx a(Re(t_0 - t))^{3/4}$ before reconnection (collision) and as $d \approx b(Re(t - t_0))^2$ after reconnection (repulsion), where t_0 is the instant of smallest separation between vortex centroids. We find that b is a constant, thus suggesting self-similarity, but a is dependent on Re. The repulsion exponent exceeds the collision exponent because the bridge curvature is higher than that of the colliding vortex tubes. On changing the initial condition to the one proposed in Ref. [17] for two representative Reynolds numbers (Re=1000,4000), it was observed that the post reconnection scaling was largely unaffected whereas the collision exponent was seen to increase to 0.82 (based on two data points). This is to be expected as there is a strong dependence on the curvature of the vortex tubes. Bridge repulsion is faster than collision and is more autonomous as local induction predominates. This curvature increases with Re resulting in impulsive motion of the bridges. This acceleration is expected to play a major role in noise generation.

It is quite clear from the above discussion that viscosity is the cause of reconnection by cross-diffusion. At very high Re, accelerated circulation transfer near the reconnection time is observed as seen in Fig. 3a in the form of a rapid reduction of axial circulation. The maximum rate of change of circulation was found to scale simply as Re^1 (Fig. 4a). With increasing Re, the onset of bridging is delayed due to decreasing viscous effects, but as bridging commences, the topological rearrangement of vorticity is rapid and the reconnection process is accelerated. The reconnection time t_R (defined as the time for the axial circulation to reduce from 95% of its original value to 50%) was found to scale as $Re^{-3/4}$ (Fig. 4b). This period is chosen because at later times, the circulation transfer is considerably affected by the evolving asymmetry.

Further insight into the dynamics of the reconnection can be obtained by investigating the enstrophy and enstrophy transfer spectra as shown in Figs. 5,6. The flattening of the vortex tubes in the contact region and the simultaneous initiation of bridges and the formation of the threads (in a head-tail structure) generates enstrophy at much higher wave numbers (note the focusing of the enstrophy transfer in a narrow wave number band). The rapid development of these small-scale structures is followed by an equally rapid decay due to viscous dissipation.

Figure 7a shows the evolution of the volume averaged enstrophy production. Not unexpectedly, the peaks do not stand out in the volume average, but are seen to fit a power law (Fig. 7b) given by $Re^{1.751}$. The peak dissipation rate was also found to scale as $Re^{-0.52}$.

Figure 8 shows the λ_2 (middle eigenvalue of velocity gradient tensor) iso-surfaces for three represen-

tative *Re* at instants beyond the reconnection time. At highest *Re*, the intense stretching and high curvature of the vortex lines (near the region that connects the threads to the reconnected vortices) results in the generation of extremely thin sheet-like structures which subsequently break down into much smaller scales. The transition to an increasingly complex entanglement of vortex lines is further aggravated by the appearance of asymmetries in the $y-z$ plane. The origin of this asymmetry is shown in Fig. 9. As the threads approach each other, the cores are flattened, leading to the formation of the head-tail structure. Due to the higher concentration of vorticity, the head of the dipole advects faster than the tail, and, as a result, the dipole structure is stretched into a sheet-like structure, similar to a planar jet. The sheets then roll-up via Kelvin-Helmholtz instability, generating multiple dipoles (threads) and this highly unstable configuration ultimately gives rise to asymmetries as in a plane jet.

(a) Re=2000 (b) Re=6000

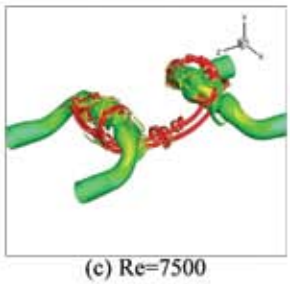

(c) Re=7500

Figure 8: λ_2 iso-surfaces (colored with vorticity magnitude) at $t \approx 4.95$

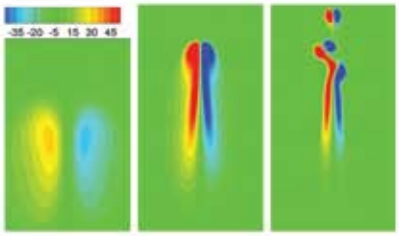

(a) t=2.95 (b) t=3.45 (c) t=3.95

Figure 9: Contours of axial vorticity for Re=6000 (slice through the dividing plane)

In this work, we have elucidated the mechanism of viscous vortex reconnection and quantitative and qualitative effects of Reynolds number are documented. We believe that our findings would be useful in the development of theories of turbulent cascade, mixing and aerodynamic noise. These phenomena can be explored in greater depth at much higher Reynolds numbers, which are beyond currently available computational resources.

References

[1] Bewley, G.P., Paoletti, M.S., Sreenivasan, K.R., and Lathrop, D.P., "Characterization of reconnecting vortices in superfluid helium," *PNAS*, Vol. 105 (37), pp:13707-13710, 2008.

[2] Kida, S., and Takaoka, M., "Vortex reconnection," *Ann. Rev. Fl. Mech.*, Vol. 26, pp: 169-189, 1994.

[3] Laufer, J., and Yen, T.-C., "Noise generation by a low-Mach number jet," *J. Fl. Mech.*, Vol. 134, pp: 1-31, 1984.

[4] Kibens, V., "Discrete noise spectrum generated by an acoustically excited jet," *AIAA J.*, Vol. 18, pp:434-451, 1979.

[5] Ffowcs Williams, J.E., and Kempton, A.J., "The noise from the large-scale structure of a jet," *J. Fl. Mech.*, Vol. 84, pp:673-694, 1978.

[6] Crighton, D.G., “The excess noise field of subsonic jets,” *J. Fl. Mech.*, Vol. 56, pp:683-694, 1972.

[7] Zaman, M.Q., and Hussain, M.F., “Vortex pairing in a circular jet under controlled excitation, Part 1: General jet response,” *J. Fl. Mech.*, Vol. 101, pp:449-491, 1980.

[8] Zaman, M.Q., and Hussain, M.F., “Turbulence suppression in free shear flows by controlled excitation,” *J. Fl. Mech.*, Vol. 103, pp: 133-159, 1981.

[9] Hussain, M.F., “Coherent structures âŁ“ reality and myth,” *Phys. Flds.*, Vol. 26 (10), pp: 2816-2850, 1983.

[10] Hussain, M.F., “Coherent structures and turbulence,” *J. Fl. Mech.*, Vol. 173, pp: 303-356, 1986.

[11] Ashurst, W.I., and Meiron, D.I., “Numerical study of vortex reconnection,” *Phys. Rev. Lett.*, Vol. 58, pp:1632âŁ“1635, 1987.

[12] Shelley, M.J., Meiron, D.I., and Orszag, S.A., “Dynamical aspects of vortex reconnection of perturbed anti-parallel vortex tubes,” *J. Fl. Mech.*, Vol. 246, pp:613-652, 1993.

[13] Boratav, O.N., Pelz, R.B., Zabusky, N.J., “Reconnection in orthogonally interacting vortex tubes: Direct numerical simulations and quantifications,” *Phys. Flds. A*, Vol. 4, pp:581-605, 1992.

[14] Kida, S., Takaoka, M., and Hussain, M.F., “Collision of two vortex rings,” *J. Fl. Mech.*, Vol. 230, pp:583-646, 1991.

[15] Melander, M. V., and Hussain, M.F., “Cut-and-connect of two antiparallel vortex tubes,” *Stanford CTR Summer Rep.*, pp:257-286, 1988.

[16] Pradeep, D.S., and Hussain, M.F., “Effects of boundary condition in numerical simulations of vortex dynamics,” *J. Flu. Mech.*, Vol. 516, pp:115-124, 2004.

[17] Bustamante, M., and Kerr, R.M., “3D Euler about a 2D symmetry plane,” *Nonlin. Phenomena*, Vol. 237, pp:1912-1920, 2008.

[18] Grafke, T., Homann, H., Dreher, J., and Grauer, R., “Numerical simulations of possible finite time singularities in the incompressible Euler equations,” *Nonlin. Phenomena*, Vol. 237, pp:1932-1936, 2008.